Taylor & Francis
Taylor & Francis Group

LABORATORY STUDY

Tamibarotene inhibit the accumulation of fibrocyte and alleviate renal fibrosis by IL-17A

Lixi Li*, Ran Luo*, Yi Yang, Yichun Cheng, Shuwang Ge and Gang Xu

Department of Nephrology, Tongji Hospital Affiliated to Tongji Medical College, Huazhong University of Science and Technology, Wuhan, China

ABSTRACT

Renal fibrosis is a common pathological process in the progression of chronic kidney disease. Accumulating evidence suggests that interleukin-17A (IL-17A) and fibrocytes play crucial roles in the pathogenesis of fibrosis. However, the role of IL-17A in the regulation of renal fibrocytes in renal fibrosis has rarely been reported. Here, we report that the plasma IL-17A level is increased in immunoglobulin A nephropathy (IgAN) patients and is correlated with clinical parameters. Using a mouse model of unilateral ureteral obstruction (UUO), we found that both IL-17A expression and fibrocyte infiltration were increased in the kidneys of UUO mice. Besides, IL-17A enhanced fibrosis and fibrocyte-associated chemokine and activator expression *in vitro*. Furthermore, inhibition of IL-17A using Am80 (Tamibarotene) decreased fibrocytes and fibrocyte-associated chemokine and activator expression and significantly attenuated renal fibrosis in the UUO mice. Our findings suggest that Am80, which inhibits the accumulation of fibrocytes and alleviates renal fibrosis mediated by IL-17A, maybe a novel therapeutic drug for renal fibrosis.

Introduction

Renal fibrosis is a common pathological process during the progression of chronic kidney disease (CKD) to end-stage renal disease. CKD places a significant burden on public health worldwide [1]. Therefore, effective treatment strategies to prevent the progression of renal fibrosis are essential for the treatment of CKD. However, the pathogenesis of renal fibrosis is not fully elucidated. It was reported that renal injury induces persistent inflammatory cell infiltration, activation of myofibroblasts, and deposition of large amounts of extracellular matrix (ECM), which eventually lead to renal fibrosis [2]. Tubular epithelial–mesenchymal transition and endothelial–mesenchymal transition, pericytes, renal derived fibroblasts, and circulating fibrocytes have all been proposed as potential sources of myofibroblasts, which are responsible for the production of ECM during renal fibrosis [3].

Circulating fibrocytes are bone marrow-derived mesenchymal cells, which express markers of hematopoietic cells, leukocytes, and fibroblasts [4]. Bucala et al.

showed that circulating fibroblasts differentiated from monocytes under the regulation of platelet-derived growth factor (PDGF) and semaphorin 7A and that CXCL12 promotes the migration of fibrocytes to injured tissues and organs through peripheral circulation [5]. Under the regulation of various cytokines present in the local microenvironment, fibrocytes gradually lose the surface markers of mesenchymal cells, such as CD34 and CD45, and differentiate into myofibroblasts by expressing α-SMA, fibronectin (FN), and collagen I (Col I), and participate in renal fibrosis [6]. However, the specific mechanism of the regulation of fibrocyte accumulation remains unclear.

Accumulating evidence suggests that IL-17A plays a crucial role in the pathogenesis of fibrosis. Increased production of IL-17A was observed in patients with advanced liver fibrosis and diffuse systemic sclerosis [7,8]. The role of IL-17A in renal fibrosis is contradictory. Sun et al. have shown that IL-17A acts as an inhibitory factor in TGF-β-induced renal fibrosis in UUO model [9], but Peng et al. have reported that IL-17A contributes significantly to the pathogenesis of renal fibrosis by

regulating RANTES-mediated inflammatory cell infiltration [10]. IL-17RA was found to modulate monocyte subsets and macrophage generation in renal fibrosis in Il17ra$^{(-/-)}$ mice [11]. Hayashi et al. found that IL-17A mediates the proliferation of fibrocytes through CD40, while it strengthens the expression of Col I in fibrocytes and participates in pulmonary fibrosis [12]. Fleige et al. reported that IL-17A upregulates CXCL12 in mice with pulmonary infection [13]. However, the role of IL-17A in the regulation of renal fibrocytes in renal fibrosis has rarely been reported.

Retinoic acid, a metabolite of vitamin A, has been reported to alleviate the fibrotic response in lung, liver, and heart injuries in vivo [14–16]. Compared to all-trans retinoic acid, AM80 is a synthetic retinoic acid that has higher stability and fewer potential adverse reactions, and it has been reported to ameliorate fibrosis in bleomycin-induced dermal fibrosis [17]. More importantly, Am80 which also has a 'generic' pharmaceutical name of Tamibarotene has been used in the treatment of acute promyelocytic leukemia in the clinic and is considered a candidate drug for the prevention of Alzheimer's disease [18,19]. The majority of Am80-mediated protective effects depend on the inhibition of Th17 [20]. Whether Am80 has beneficial effects in renal fibrosis remains unknown.

To evaluate the clinical significance of IL-17A, we analyzed the clinical parameters of immunoglobulin A nephropathy (IgAN) patients along with the level of plasma IL-17A. We established unilateral ureteral obstruction (UUO) models to investigate the expression of IL-17A and the infiltration of fibrocytes during kidney injury. For further analysis of the activation and regulation of fibrocytes by IL-17A in renal fibrosis, we used recombinant IL-17A to stimulate renal tubular cells in vivo and inhibited IL-17A expression using Am80 to alter fibrocytes in UUO models.

Methods

Blood sample from IgAN patients and normal subjects

Eighty-eight patients (51 men and 37 women; mean age = 36.78 ± 1.09 years) who underwent kidney biopsy and pathologic diagnosis of IgAN between January 2012 and December 2014 at the Tongji Hospital were enrolled in the study. Their blood samples were obtained at the time of diagnosis. The exclusion criteria included age <18 years and secondary etiologies of IgAN (anaphylactoid purpura and liver cirrhosis among others). Our protocol was approved by the institutional review board or ethics committee at Tongji hospital.

Written informed consent was obtained from all patients.

Cell culture

We followed the methods reported by Xu et al. for cell culture [21]. A 6-well assay plate precoated with anti-CD3 and anti-CD28 Ab (BD Pharmingen) was incubated at 37 °C for 4 h. Splenocytes (1×10^6 cells/well) were obtained from the spleens of 3 to 4-weeks-old mice and cultured for 3 d in 6-well plates in a medium containing TGF-β (2 ng/mL; Peprotech), IL-6 (20 ng/mL; Peprotech), anti-IFN-γ (10 μg/mL; eBioscience), and anti-IL-4 (10 μg/mL; eBioscience). These cells were treated with DMSO or Am80 (1 or 10 nmol/L) for 72 h and then collected for the Th17 cell differentiation test using flow cytometry, while the cell supernatants were used for the detection of IL-17A using enzyme-linked immunosorbent assay (ELISA).

The rat renal tubular epithelial cell line, NRK-52E, was purchased from GuangZhou Jennio Biotech and cultured in F12/DMEM (Hyclone) with 10% fetal calf serum (GIBCO). After pre-incubation in F12/DMEM without serum for 8 h, the NRK-52E cells were treated with PBS, TGF-β (10 ng/mL; Peprotech), IL-17A (10 ng/mL; Peprotech), or TGF-β (10 ng/mL) + IL-17A (10 ng/mL) for 48 h.

UUO model

The UUO model was constructed following the method reported by Xu et al. [21]. Male C57BL/6 mice were purchased from Hua Fukang Experimental Animal Center (Beijing, China) and maintained under specific pathogen-free conditions. UUO, a typical animal renal injury, was induced through a flank incision on the back of the mice (aged 7–9 weeks). The left ureter was exposed and tied off with two 4.0 silk sutures and permanently ligated. Sham-operated mice underwent an identical procedure, but without the ureteric ligation. After 7 days, the mice were euthanized, and their obstructed kidney tissues and peripheral blood were collected. The therapeutic experiment with Am80 (LKT Laboratories, Shanghai, China) was performed by intragastric administration of 1 mg/kg Am80 in U + A1 group and 2 mg/kg Am80 in the U + A2 group to the mice starting on day 1 following UUO induction and daily until the mice were euthanized; the mice that received hydroxymethyl cellulose (CMC) only served as the disease control (U + C) group.

Pathological, IHC, and immunofluorescence evaluations

Paraffin-embedded renal sections (4 μm) were subjected to Masson's trichome and Sirius red staining, as reported previously. Paraffin-embedded renal sections (4 μm) were deparaffinized in xylene and rehydrated in graded alcohol. The endogenous peroxidase activity was blocked with 3% H_2O_2 at room temperature for 15 min, and nonspecific proteins were blocked with 10% goat serum for 30 min. The sections were then incubated overnight with an antibody against α-SMA (Abcam, Cambridge, MA) at 4 °C, followed by incubation with an HRP-conjugated secondary antibody; subsequently, they were visualized with diaminobenzidine substrate and hematoxylin counterstaining. For double-labeling immunofluorescence studies, following incubation with the primary antibody against F4/80 (Abcam, Cambridge, MA), the sections were incubated with FITC-conjugated secondary antibody. The nucleus was counterstained with DAPI. Color images were obtained under a Nikon fluorescence microscope (Nikon ECLIPSE TE2000-U, Tokyo, Japan).

Real-time PCR assay

Real-time PCR was performed as described previously [22]. Real-time PCR was carried out using the LightCycler 480 system (Roche, Pleasanton, CA), with the following primers: IL17A, forward 5′-TTTAACTCCC TTGGCGCAAAA-3′, reverse 5′-CTTTCCCTCCGCATTGA CAC-3′; CXCL12, forward 5′-TGCATCAGTGACGGTAAAC CA-3′, reverse 5′-CACAGTTTGGGAGTGTTGAGGAT-3′; Fibronectin, forward 5′-ATGTGGACCCCTCCTGATAGT-′, reverse 5′-GCCCAGTGATTTCAGCAAAGG-3′; Collagen 1, forward 5′-GCTCCTCTTAGGGGGCCACT-3′, reverse 5′-ATT GGGGACCCTTAGGCCAT-3′; GAPDH, forward 5′-TCCGC CCCTTCTGCCGATG-3′, reverse 5′-CACGGAAGGCCATGCC AGTGA-3′; TGF-β1, forward 5′-CGCAACAACGCCATCTA TGA-3′, reverse 5′-ACCAAGGTAACGCCAGGAAT-3′; The fold change of expression compared to the expression in the control was calculated using the formula $2^{-\Delta\Delta Ct}$.

ELISA

IL-17A protein levels in the mouse or human blood and cell supernatants were detected using a commercial IL-17A Quantikine ELISA Kit (Westing Biotech, Shanghai, China) according to the manufacturer's instructions. The CXCL12 protein level in the mouse blood was detected using a commercial CXCL12 Quantikine ELISA Kit (Westing Biotech, Shanghai, China) according to the manufacturer's instructions.

Western blot analyses

Western blotting was performed, and results were analyzed as described previously [23]. The following primary antibodies were used at the indicated dilutions: GAPDH (1:3000, mouse, Santa Cruz), PDGF-BB, Col I, semaphorin7A, CXCL12, and α-SMA (all at 1:2000, Abcam, Cambridge, MA). The membranes were then incubated with the appropriate horseradish peroxidase (HRP)-conjugated secondary antibody, and the target signals were detected using the ECL Plus Western Blot Kit (Amersham Pharmacia Biotech, NJ).

Flow cytometry

Flow cytometry was performed following the method reported by Xu et al. [21]. A single-cell suspension of the renal cells was prepared and incubated with a primary antibody or the appropriate isotype control antibody at 4 °C for 30 min. The following antibodies were used: FITC-conjugated anti-mouse CD45 (Biolegend), APC-conjugated anti-mouse Collagen I (Biolegend), FITC-conjugated anti-mouse CD4 (eBioscience), and PE-cy7-conjugated anti-mouse IL-17A (BioGems) antibodies. All flow cytometric analyses were performed using an LSR II Flow Cytometer (Beckman–Coulter) and the Flowjo software.

Statistical analyses

Statistical analyses and power calculations were carried out using the SPSS 23.0 software (SPSS, Chicago, IL) and GraphPad Prism version 7 software (Graph software, San Diego, CA). Correlations were evaluated using non-parametric Spearman's and parametric Pearson's correlation tests. Cox regression was used to analyze the association between the plasma IL-17A level and renal outcome. Statistical analyses using Student's t-test or one-way ANOVA were performed where applicable. All the statistical analyses were two-tailed. $p < 0.05$ was considered statistically significant.

Results

Increased IL-17A levels were observed in the blood samples from IgAN patients

Eighty-eight patients who were diagnosed with IgAN through observation of renal biopsy specimens were recruited for the study. The initial estimated glomerular filtration rate (eGFR) of the eighty-eight patients was 62.75 mL/min/1.73 m² (12.94–223.57), while that of normal controls was 102.20 mL/min/1.73 m² (77.82–132.85)

Table 1. Demographic and clinical characteristics of IgAN patients.

Characteristics	IgAN patients ($n = 88$)	Control ($n = 45$)
Baseline		
Age (years; mean ± SD)	36.78 ± 10.21	33.14 ± 1.33
Gender (male/female)	51/37	24/21
SBP (mmHg; mean ± SD)**	132.02 ± 18.63	122.55 ± 2.72
DBP (mmHg; mean ± SD)*	85.24 ± 13.57	80.53 ± 2.45
Hypertensive subjects (%)	35 (39.77%)	11 (17.78%)
Macro hematuria (%)	6(6.82%)	
Proteinuria (g/d; median, IQR)	1.13 (0.13–16.96)	
Scr (μmol/L; median, IQR)*	120 (54–395)	68 (52–89)
eGFR (mL/min per 1.73 m²; median, IQR)**	62.75 (12.94–223.57)	102.20 (77.82–132.85)
CKD stages (%)		
1	20.45	
2	31.82	
3	42.05	
4	4.55	
5	1.14	

Values are expressed as mean ± standard deviation, median (25th percentile to 75th percentile), or number (percentage). eGFR was calculated with CKD-EPI equation.
SBP: systolic blood pressure; DBP: diastolic blood pressure; Scr: serum creatinine; eGFR: estimated glomerular filtration rate; IQR: interquartile range.
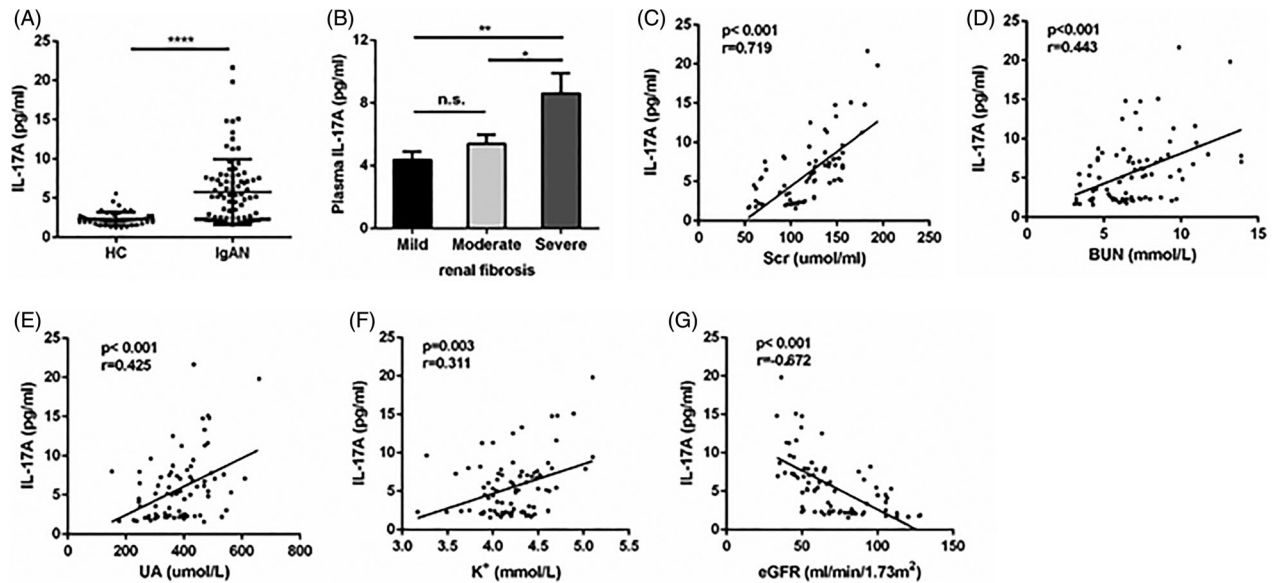*$p < 0.05$; **$p < 0.01$.

Figure 1. Plasma IL-17A levels correlated with clinical parameters. Comparison of plasma IL-17A levels between healthy controls ($n = 45$) and IgAN patients ($n = 88$) (A). Relationship between plasma IL-17A and with the degree of renal fibrosis (B). Correlations between plasma IL-17A level and Scr (C), BUN (D), UA (E), serum K+ (F), and eGFR (G) through univariate analysis.

($p < 0.01$) (Table 1). The clinical parameters, including age, gender, and hypertension, were not different between the IgAN cohort and the normal controls. Out of the eighty-eight patients, gross hematuria at onset was present in six (6.82%) and hypertension was present in thirty-five (39.77%) patients. As shown in Figure 1(A), the plasma IL-17A level was increased in the IgAN patients compared to that in the normal controls. In addition, along with enhanced renal fibrosis, plasma IL-17A increased significantly in IgAN patients (Figure 1(B)). Further, the plasma IL-17A level was significantly positively correlated to serum creatinine ($p < 0.001$) (Figure 1(C)), blood urea nitrogen ($p < 0.001$)

(Figure 1(D)), uric acid ($p < 0.001$) (Figure 1(E)), and serum K+ ($p = 0.003$) (Figure 1(F)) but significantly negatively correlated to eGFR ($p < 0.001$) (Figure 1(G)). These results suggested that the increased production of IL-17A in the IgAN patients was involved in decreasing the renal function in these patients.

Increased IL-17A expression and fibrocyte infiltration were observed in the kidney of UUO mice

In our previous study, we have reported that the proportion of Th17 cells increased in the UUO model of

the kidney [21]. We used the UUO mouse model to investigate the expression of IL-17A and the infiltration of fibrocytes into the injured kidney. As shown in Figure 2(A), the level of plasma IL-17A was significantly increased in the UUO mice compared to that in the sham control mice. Furthermore, the renal mRNA level of IL-17A was also markedly increased in the UUO mice compared to that in the sham control mice (Figure 2(B)). FACS results revealed that CD45+/Collagen I+ double-positive fibrocytes constituted 8.55% of the fibroblasts in the UUO mice, whereas in sham control

mice they constituted 0.63% of the fibroblasts. The proportion of these fibroblasts in the kidneys of the UUO group was significantly higher than that in the kidneys of the sham control group (Figure 2(E,F)). Besides, the plasma level of the fibrocyte-related chemokine, CXCL12, was increased in the UUO mice compared to that in the sham control mice, and the renal mRNA level of CXCL12 was also increased in the UUO mice compared to that in the sham control mice (Figure 2(C,D)). Western blotting showed that compared to that in the sham-operated group, the expression levels of
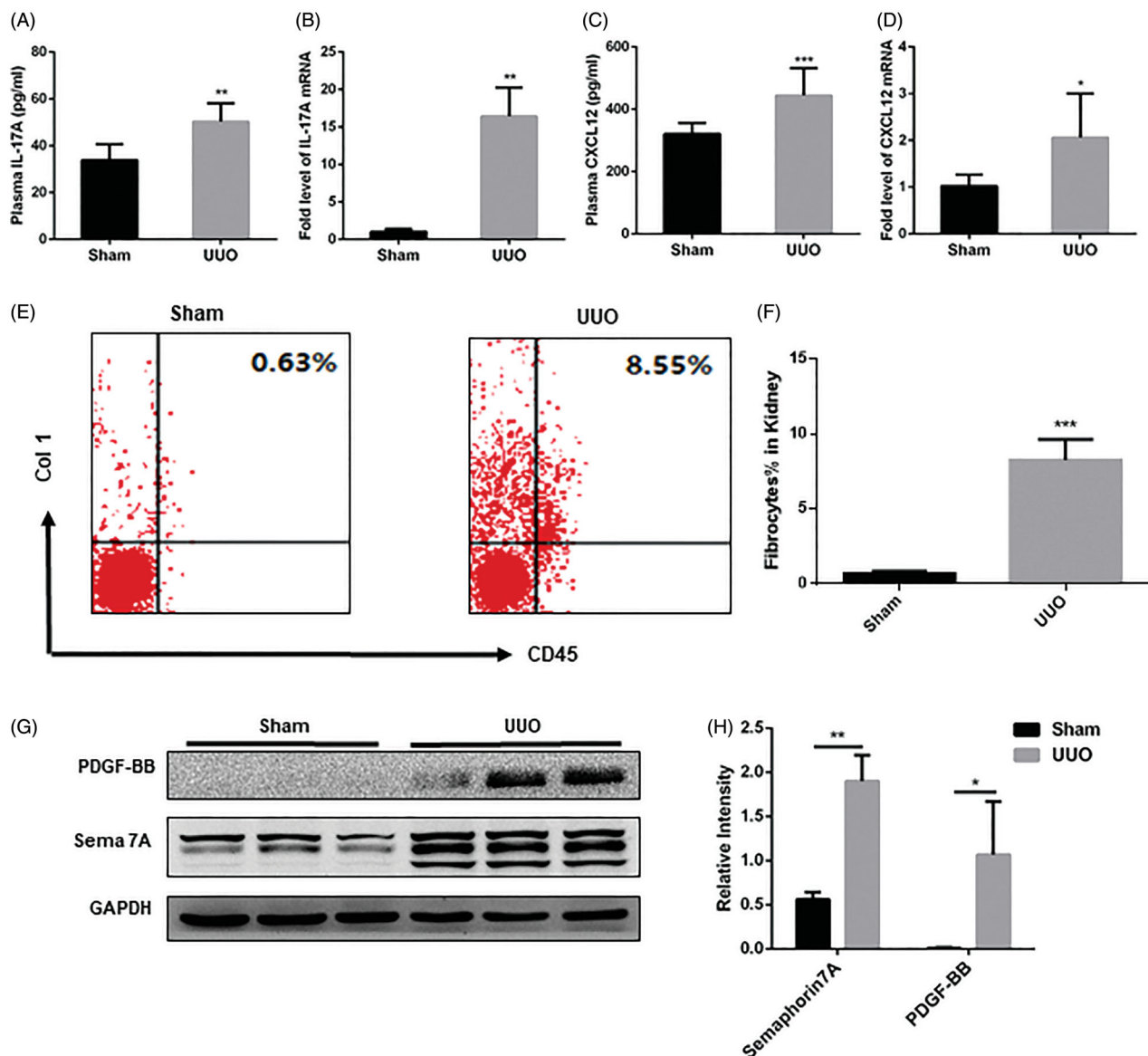

Figure 2. IL-17A expression and fibrocyte infiltration increased in the kidneys of UUO mice. Histograms showing the plasma levels of IL-17A (A) and CXCL12 (C), in the sham and UUO groups ($n = 3$ per group). RT-PCR for mRNA levels of IL-17A (B) and CXCL12 (D) in sham and UUO mouse kidneys ($n = 3$ per group). Representative flow cytometry biaxial plots (E) and statistical summary (F) of CD45+/Collagen I+ fibrocyte cells gate from renal single cell suspension of sham and UUO mice ($n = 3$ per group). Expression levels of PDGF-BB and Sema 7A were detected by western blotting (G), and the histogram (H) shows the relative intensity for each marker normalized to the intensity for GAPDH of sham and UUO kidney ($n = 3$ per group). $*p < 0.05$; $**p < 0.01$; $***p < 0.001$.

the fibroblast-associated activators, semaphorin7A and PDGF-BB, were strikingly increased in the UUO model group (Figure 2(G,H)). In the contralateral kidney of sham and UUO mice, the relative expression of fibrosis and fibrocytes-associated chemokine has no significant difference (Figure S1(A,B)). These results suggest that IL-17A and fibrocytes are increased in the kidney following UUO.

IL-17A enhanced fibrosis and fibrocyte-associated chemokine and activator expression in vitro

To assess the role of IL-17A in renal fibrosis, we used recombinant IL-17A to stimulate NRK-52E cells. TGF-β was used to stimulate NRK-52E as a positive control. Western blotting results showed that the expression of FN, α-SMA, and Col 1 was significantly increased in the

TGF-β-, IL-17A-, and TGF-β + IL-17A-treated groups compared to that in the PBS treated group (Figure 3(A,B)). Besides, the western blotting results also showed that the expression of CXCL12, semaphorin7A, and PDGF-BB was significantly increased in the TGF-β, IL-17A, and TGF-β + IL-17A groups compared to that in the PBS group (Figure 3(C,D)). These results demonstrated that IL-17A was involved in fibrocyte-related chemokine and activator expression.

Am80 attenuated renal fibrosis in UUO mice by regulating epithelial-mesenchymal transition (EMT) and myofibroblasts

To explore the contribution of IL-17A in the pathogenesis of UUO, we used Am80 to block IL-17A activation. Our experiment demonstrated the inhibitory effect of
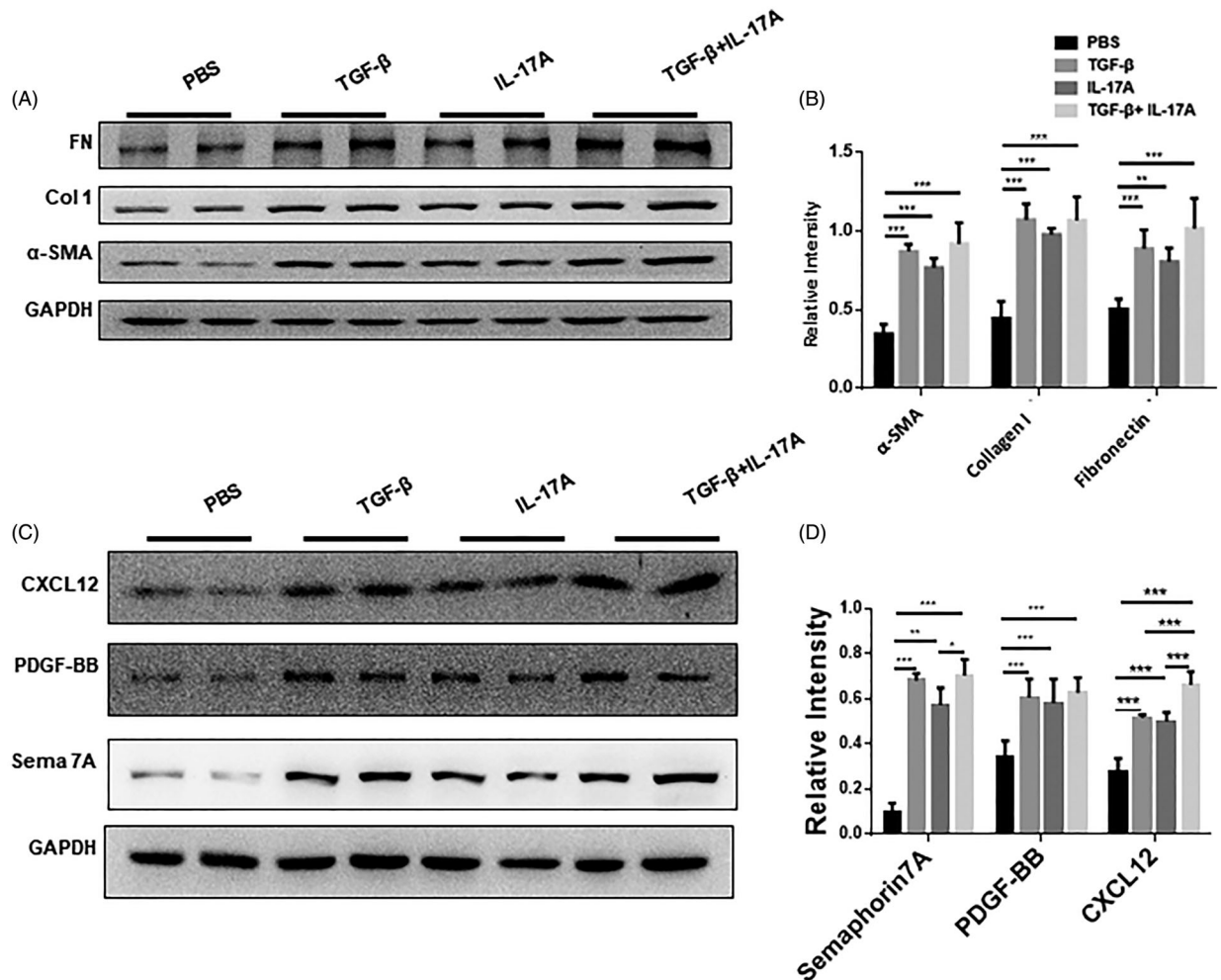

Figure 3. IL-17A enhanced fibrosis and fibrocyte-associated chemokine and activator expression of NRK-52E cells *in vitro*. Expression levels of FN, Col 1, and α-SMA in PBS, TGF-β (10 ng/mL), IL-17A (10 ng/mL), and TGF-β (10 ng/mL) + IL-17A (10 ng/mL) treatment (48 h) groups ($n = 5$ per group) were detected by western blot analysis (A), and the histogram (B) shows the relative intensity of each marker normalized to the intensity for GAPDH. Expression levels of the CXCL12, PDGF-BB, Sema 7A in PBS, TGF-β (10 ng/mL), IL-17A (10 ng/mL), and TGF-β (10 ng/mL) + IL-17A (10 ng/mL) treatment groups (48 h) ($n = 5$ per group) were detected by western blot analysis (C), and the histogram (D) shows the relative intensity of each marker normalized to the intensity of GAPDH. FN: fibronectin; Col 1: collagen 1. $*p < 0.05$; $**p < 0.01$; $***p < 0.001$.
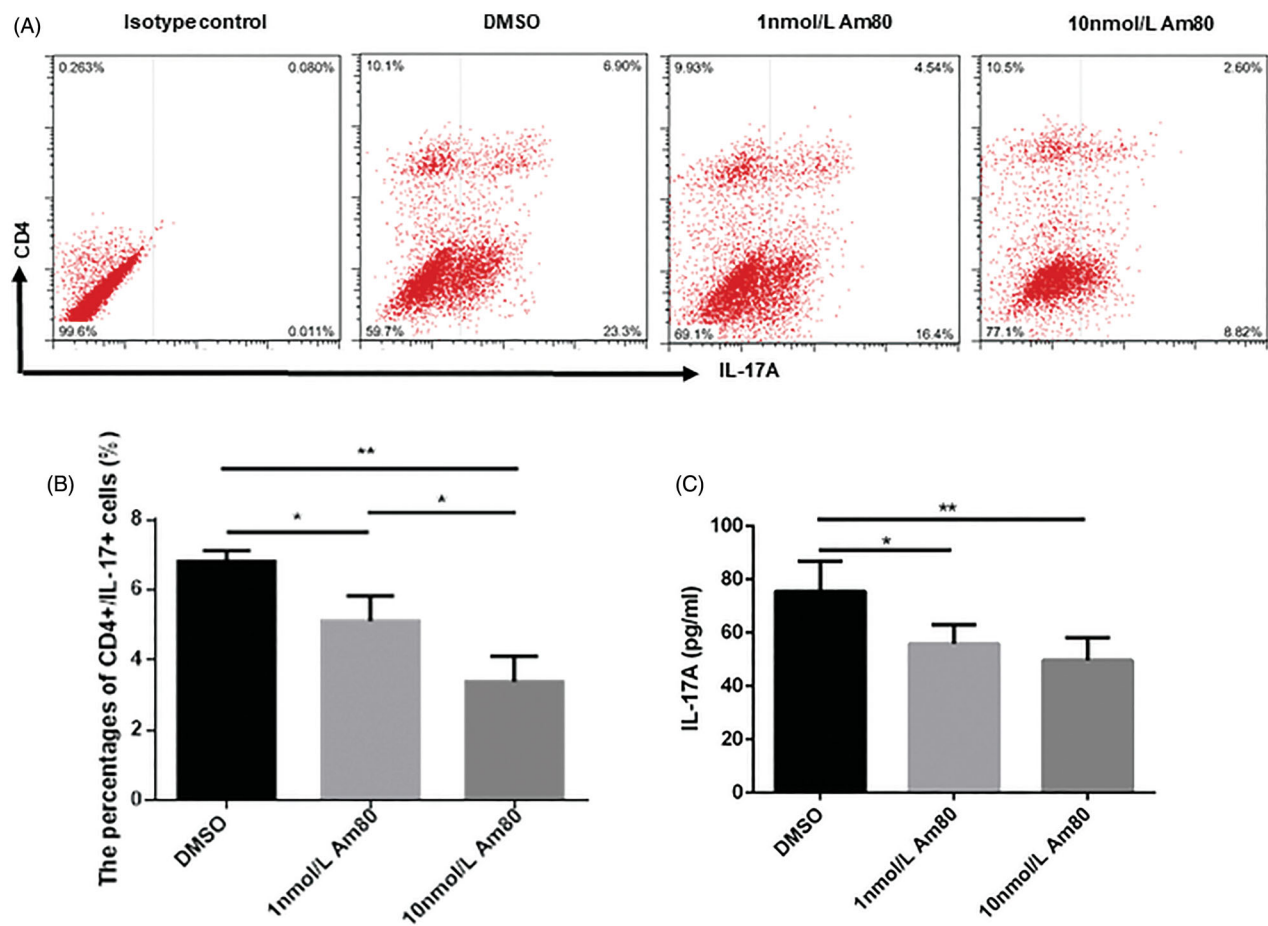
Figure 4. Effect of Am80-mediated inhibition of IL-17A in splenocytes. Representative flow cytometry biaxial plots (A) and statistical summary (B) of the CD4+/IL-17A + cells gate from spleen single cell suspension in isotype, DMSO, Am80 (1 nmol/L), and Am80 (10 nmol/L) treatment groups ($n = 3$ per group). Histograms showing levels of IL-17A in the supernatants (C) in the different treatment groups. $*p < 0.05$; $**p < 0.01$; $***p < 0.001$.

Am80 on IL-17A in splenocytes (Figure 4(A–C)). Sirius red and Masson's staining results and α-SMA expression indicated that UUO mice with intragastric administration of 1 or 2 mg/kg Am80 had noticeably less severe interstitial fibrosis than UUO mice administered the control vehicle (Figure 5(A–E)). Western blotting results showed that the FN, Col I, and α-SMA levels were decreased in the UUO mice following intragastric administration of Am80 (Figure 5(F,G)). Real-time PCR also indicated that the expression of FN, Col I, and α-SMA was markedly reduced in the UUO mice upon Am80 intragastric administration (Figure 5(H–J)). These results indicated that Am80 improved renal fibrosis by regulating EMT and myofibroblasts in UUO mice.

Inhibition of IL-17A by Am80 decreased fibrocytes and fibrocyte-associated chemokine and activator expression in vivo

To demonstrate the inhibitory effect of IL-17A on fibrocytes, we analyzed the fibrocytes and the expression of fibrocyte-associated chemokines and activators in UUO mice following intragastric administration of Am80. The plasma levels of IL-17A and IL-17A mRNA expression in the renal tissues were decreased in the UUO mice following intragastric administration of Am80 compared to those after administration of the control vehicle (Figure 6(A,B)). FACS results revealed that the proportions of CD45+/Collagen I + double-positive fibrocytes were 4.71% and 2.97% in the UUO mice following intragastric administration of 1 and 2 mg/kg Am80, respectively, whereas it was 6.97%. in the mice administered the vehicle control. The proportion of fibrocytes in the kidneys of the Am80-treated group of UUO mice was significantly decreased compared to that in the control vehicle-treated group (Figure 6(E,F)). Moreover, the plasma level and renal mRNA expression of the chemokine CXCL12 were decreased in the UUO mice following the intragastric administration of Am80 compared to those in UUO mice administered the vehicle control (Figure 6(C,D)). Western blotting showed that the expression of the fibroblast-associated activators,

semaphorin7A and PDGF-BB, was markedly decreased in the UUO mice following intragastric administration of Am80 compared to that following the intragastric administration of the vehicle control (Figure 6(G,H)). Taken together, these results indicated that Am80 blocks the IL-17A-mediated infiltration of fibrocytes into the kidney in response to renal injury.

Discussion

In this study, we explored the correlation between plasma IL-17A levels and clinical parameters in IgAN patients. We found that IL-17A expression and fibrocyte infiltration were increased in the UUO model compared to those in the normal controls. Through in vitro studies, we demonstrated that IL-17A directly enhances the expression of fibrosis markers and fibrocyte-associated chemokines and activators in NRK-52E cells. Reduction in IL-17A secretion following treatment with Am80 led to a significant alleviation in renal fibrosis induced post-UUO injury. Moreover, the infiltration of fibrocytes into the kidney and the expression of fibrocyte-associated chemokines and activators in response to renal injury were decreased after treatment with Am80.

Previous studies have indicated that a high baseline serum IL-17A level predicts an unfavorable histopathological response in lupus nephritis [24]. Furthermore, an imbalance of Treg/Th17, observed in IgAN patients, may play a role in the IgANpathogenesis [25]. Our previous work also showed that complement C3 produced by macrophages promotes renal fibrosis through the secretion of IL-17A [21]. IL-17A plays a vital role in renal pathogenesis. Here, we showed that the plasma levels of IL-17A were significantly higher in IgAN patients and in the UUO mice model, compared to those in normal controls and sham group, which is consistent with the previous clinical report and elevated levels of circulating cytokines in other UUO model, such as, IL-1β, IL-6, and TNF-α [26]. Additionally, our data showed that plasma IL-17A concentrations were significantly positively correlated with Scr, BUN, and UA and significantly negatively correlated with eGFR. These results suggested that IL-17A plays an important role in the development of the renal disease. Besides, Lin et al. found that serum IL-17A correlated with 24 h proteinuria in IgAN patients [25]. The lack of data pertaining to 24 h proteinuria in our cohort was the reason why we were unable to observe the relationship between IL-17A and 24 h proteinuria.

Recently, an increasing number of studies have confirmed that fibrocytes are associated with the pathological process of fibrosis of various tissues and organs, such as pulmonary, hepatic, cardiac, and skin fibrosis [27–30]. The CXCR4/CXCL12 axis is the main driving force for fibrocyte transport. A previous study reported that anti-CXCL12 antibodies significantly reduce the aggregation of fibrocytes in lung tissues and alleviate pulmonary fibrosis in animal models of pulmonary fibrosis [31]. Moreover, neutralization of IL-17A significantly reduces the expression of CXCL12 in animal models of breast cancer-associated metastasis [32]. Our results showed that the accumulation of fibrocytes and production of the fibrocyte-related chemokine, CXCL12, and activating factors, Semaphorin7A and PDGF-BB, were significantly increased in the kidney of the UUO model. Furthermore, we found that IL-17A directly facilitates the production of fibrocyte-related chemokine and activating factors by tubular cells. These results suggest that the recruitment and activation of fibrocytes in the renal fibrosis process may be regulated by IL-17A.

AM80 was reported to effectively inhibit the differentiation of Th17 cells and the production of IL-17A[20]. Our results showed that Am80 effectively attenuated IL-17A production in both plasma and tissues. In addition, Am80 reduced the accumulation of fibrocytes and production of fibrocyte-related chemokines and activators in the renal tissues of UUO mice, which is consistent with a previous study showing that Am80 ameliorates bleomycin-induced dermal fibrosis by modulating the phenotypes of fibroblasts [17]. Besides, Am80 alleviated renal fibrosis not only by inhibiting fibrocytes but also by regulating EMT and myofibroblasts. AM80 is currently available as a drug, Tamibarotene, for clinical use in the treatment of several human diseases. Therefore, Am80 may potentially be used as a treatment to alleviate renal fibrosis. However, its application needs to be validated further through a clinical trial.

Conclusion

We found here, a clinical correlation between the level of plasma IL-17A and renal function and demonstrated that Am80 improves renal interstitial fibrosis by inhibiting the production of IL-17A and thereby reducing the recruitment and activation of circulating fibrocytes in the kidney of the UUO model. This is the first study to explore the role of Am80 in renal fibrosis and attempts to explain its protective mechanism against fibrosis from the perspective of circulating fibrocytes, providing a new approach for delaying the progression of renal disease to end-stage renal disease in the clinic.
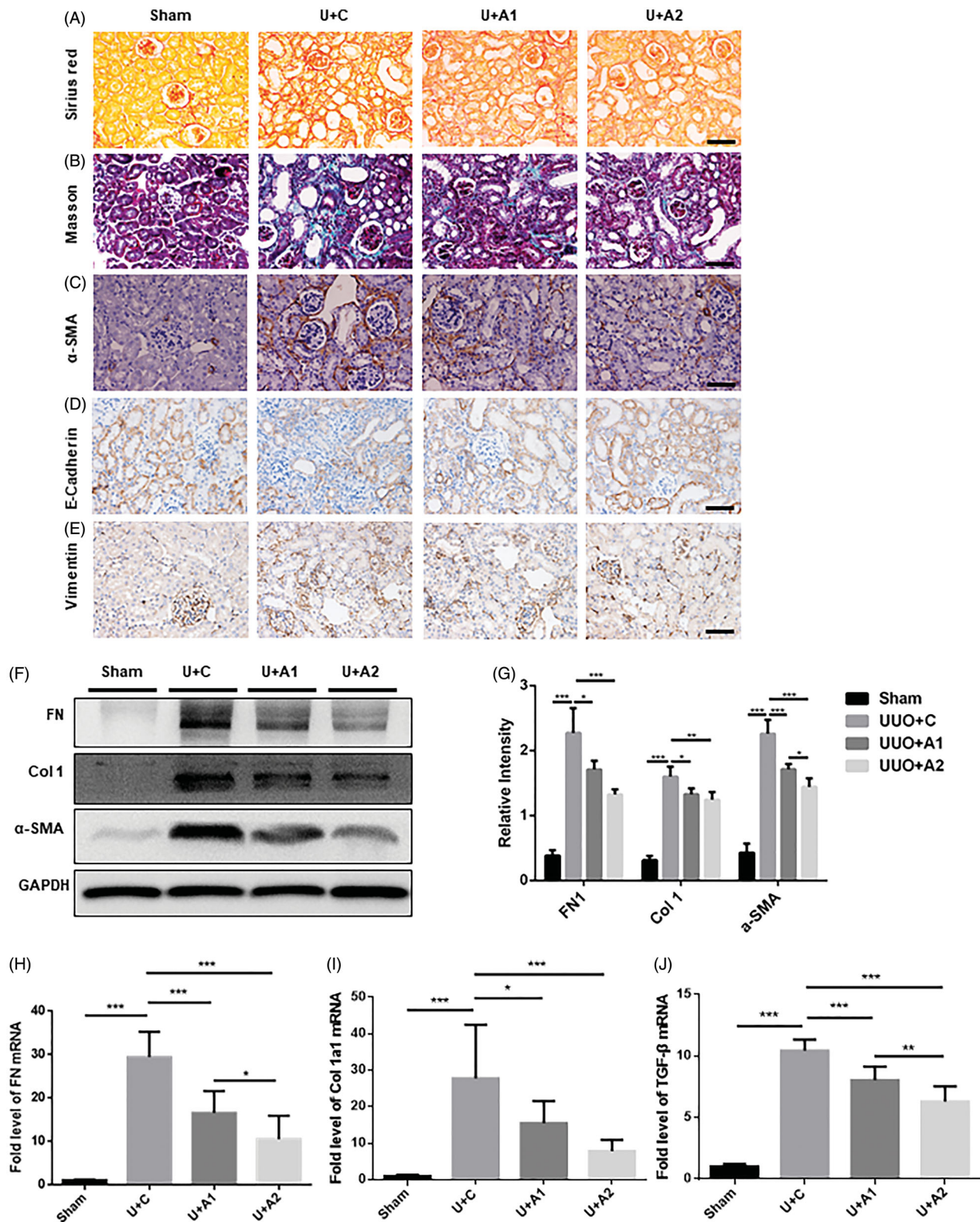
Figure 5. Am80 attenuates renal fibrosis in UUO mice. Sirius red (A), and Masson's trichrome staining (B) results showing collagen deposition. Representative image of IHC staining showing α-SMA (C), E-Cadherin (D), and Vimentin (E) expression in the UUO kidney interstitium of the sham, U + C, U + A1, and U + A2 groups. Expression levels of FN, Col 1, and α-SMA in the kidneys of the sham, U + C, U + A1, and U + A2 groups (*n* = 4 per group) were detected using western blot analysis (F), and the histogram (G) showing the relative intensity of each marker normalized to the intensity for GAPDH. RT-PCR for the kidney mRNA levels of FN (H), Col 1(I), and TGF-β (J) in the sham, U + C, U + A1, and U + A2 treatment groups (*n* = 4 per group). FN: fibronectin; Col 1: collagen 1. Bar = 50 μm, $*p < 0.05$; $**p < 0.01$; $***p < 0.001$.
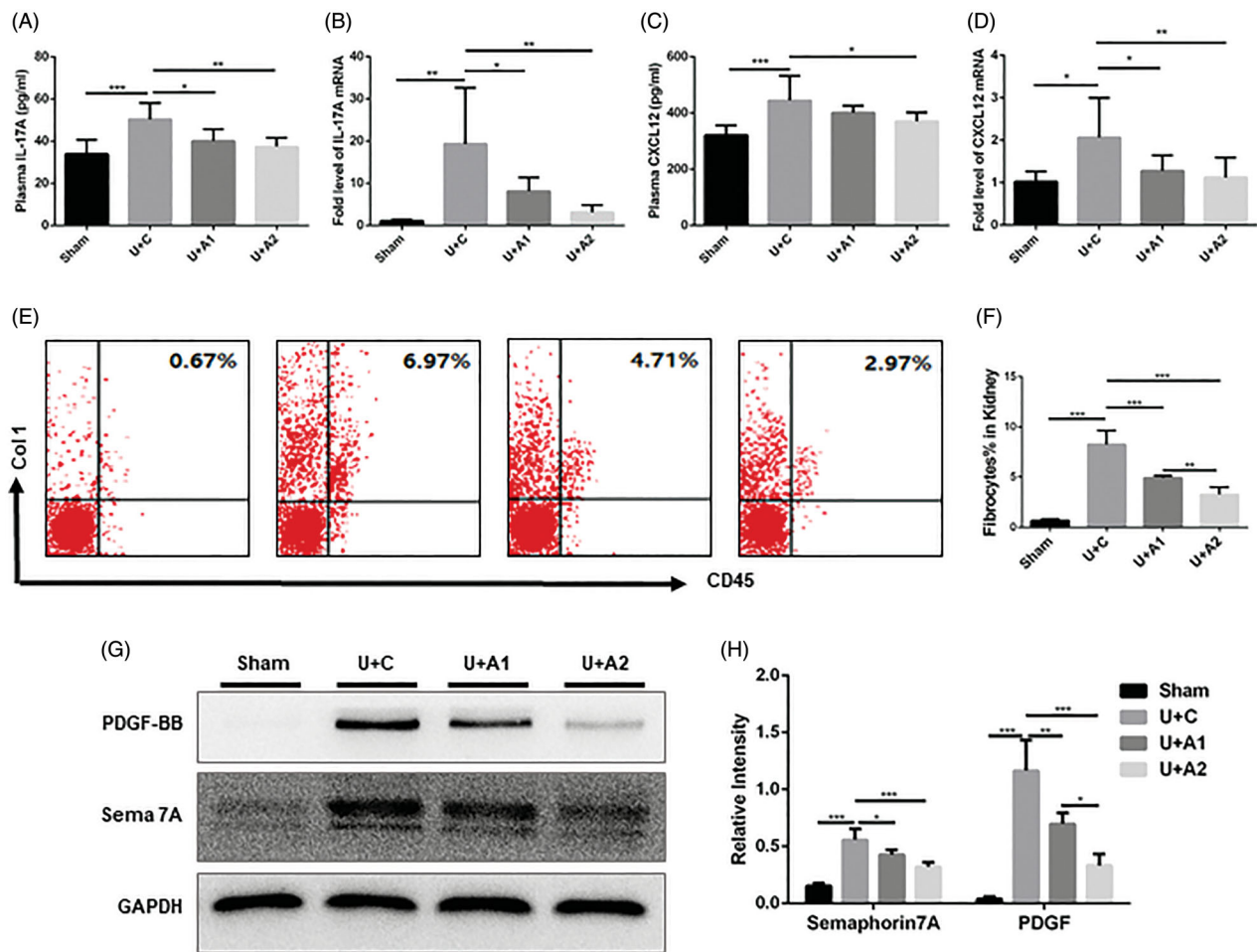
Figure 6. Inhibition of IL-17A by Am80 decreases fibrocytes and fibrocyte-associated chemokine and activator expression *in vivo*. Histograms showing the plasma levels of IL-17A (A) and CXCL12 (C) in the sham and UUO groups ($N = 4$ per group). RT-PCR for kidney mRNA levels of IL-17A (B) and CXCL12 (D) in the sham, U + C, U + A1, and U + A2 groups ($n = 4$ per group). Representative flow cytometry biaxial plots (E) and statistical summary (F) of CD45+/Collagen I + fibrocyte cells gate from renal single cell suspension of sham, U + C, U + A1, and U + A2 group mice ($n = 4$ per group). Expression levels of PDGF-BB and Sema 7A were detected by western blotting (G), and the histogram (H) shows the relative intensity of each marker normalized to the intensity for GAPDH in the kidney of sham, U + C, U + A1, U + A2 group mice ($n = 4$ per group). $*p < 0.05$; $**p < 0.01$; $***p < 0.001$.

Author contributions

G.X., S.G. designed the study. Y.C., R.L., and Y.Y. collected the clinical data. L.L. and R.L. did the experiments, prepared the figures and tables, and wrote the paper. S.G. and G.X. conceived the project and supervised and coordinated all the work.

Disclosure statement

No potential conflict of interest was reported by the author(s).

Data availability statement

The data used to support the findings of this study are included in the article.

References

[1] Webster AC, Nagler EV, Morton RL, et al. Chronic kidney disease. Lancet. 2017;389(10075):1238–1252.
[2] Andrade-Oliveira V, Foresto-Neto O, Watanabe IKM, et al. Inflammation in renal diseases: new and old players. Front Pharmacol. 2019;10:1192.

[3] Sun YB, Qu X, Caruana G, et al. The origin of renal fibroblasts/myofibroblasts and the signals that trigger fibrosis. Differentiation. 2016;92(3):102–107.

[4] Klemann C, Raveney BJ, Klemann AK, et al. Synthetic retinoid AM80 inhibits Th17 cells and ameliorates experimental autoimmune encephalomyelitis. Am J Pathol. 2009;174(6):2234–2245.

[5] Bucala R, Spiegel LA, Chesney J, et al. Circulating fibrocytes define a new leukocyte subpopulation that mediates tissue repair. Mol Med. 1994;1(1):71–81.

[6] Mori L, Bellini A, Stacey MA, et al. Fibrocytes contribute to the myofibroblast population in wounded skin and originate from the bone marrow. Exp Cell Res. 2005;304(1):81–90.

[7] Gabsi A, Heim X, Dlala A, et al. TH17 cells expressing CD146 are significantly increased in patients with Systemic sclerosis. Sci Rep. 2019;9(1):17721.

[8] Elkhawaga AA, Hosni A, Zaky DZ, et al. Association of Treg and TH17 cytokines with HCV pathogenesis and liver pathology. Egypt J Immunol. 2019;26(2):55–63.

[9] Sun B, Wang H, Zhang L, et al. Role of interleukin 17 in TGF-β signaling-mediated renal interstitial fibrosis. Cytokine. 2018;106:80–88.

[10] Peng X, Xiao Z, Zhang J, et al. IL-17A produced by both γδ T and Th17 cells promotes renal fibrosis via RANTES-mediated leukocyte infiltration after renal obstruction. J Pathol. 2015;235(1):79–89.

[11] Ge S, Hertel B, Susnik N, et al. Interleukin 17 receptor A modulates monocyte subsets and macrophage generation in vivo. PloS One. 2014;9(1):e85461.

[12] Hayashi H, Kawakita A, Okazaki S, et al. IL-17A/F modulates fibrocyte functions in cooperation with CD40-mediated signaling. Inflammation. 2013;36(4):830–838.

[13] Fleige H, Ravens S, Moschovakis GL, et al. IL-17-induced CXCL12 recruits B cells and induces follicle formation in BALT in the absence of differentiated FDCs. J Exp Med. 2014;211(4):643–651.

[14] Leem AY, Shin MH, Douglas IS, et al. All-trans retinoic acid attenuates bleomycin-induced pulmonary fibrosis via downregulating EphA2-EphrinA1 signaling. Biochem Biophys Res Commun. 2017;491(3):721–726.

[15] Hisamori S, Tabata C, Kadokawa Y, et al. All-trans-retinoic acid ameliorates carbon tetrachloride-induced liver fibrosis in mice through modulating cytokine production. Liver Int. 2008;28(9):1217–1225.

[16] Manolescu DC, Jankowski M, Danalache BA, et al. All-trans retinoic acid stimulates gene expression of the cardioprotective natriuretic peptide system and prevents fibrosis and apoptosis in cardiomyocytes of obese ob/ob mice. Appl Physiol Nutr Metab. 2014;39(10):1127–1136.

[17] Toyama T, Asano Y, Akamata K, et al. Tamibarotene ameliorates bleomycin-induced dermal fibrosis by modulating phenotypes of fibroblasts, endothelial cells, and immune cells. J Invest Dermatol. 2016;136(2):387–398.

[18] Miwako I, Kagechika H. Tamibarotene. Drugs Today. 2007;43(8):563–568.

[19] Fukasawa H, Nakagomi M, Yamagata N, et al. Tamibarotene: a candidate retinoid drug for Alzheimer's disease. Biol Pharm Bull. 2012;35(8):1206–1212.

[20] Larange A, Cheroutre H. Retinoic acid and retinoic acid receptors as pleiotropic modulators of the immune system. Annu Rev Immunol. 2016;34:369–394.

[21] Liu Y, Wang K, Liang X, et al. Complement C3 produced by macrophages promotes renal fibrosis via IL-17A secretion. Front Immunol. 2018;9:2385.

[22] Luo R, Guo SM, Li YQ, et al. Plasma fractalkine levels are associated with renal inflammation and outcomes in immunoglobulin A nephropathy. Nephrol Dial Transplant. 2019;34(9):1549–1558.

[23] Luo R, Guo SM, Li YQ, et al. Plasma fractalkine levels are associated with renal inflammation and outcomes in immunoglobulin A nephropathy. Nephrol Dial Transplant. 2019;34(9):1549–1558.

[24] Abdel Galil SM, Ezzeldin N, El-Boshy ME. The role of serum IL-17 and IL-6 as biomarkers of disease activity and predictors of remission in patients with lupus nephritis. Cytokine. 2015;76(2):280–287.

[25] Lin FJ, Jiang GR, Shan JP, et al. Imbalance of regulatory T cells to Th17 cells in IgA nephropathy. Scand J Clin Lab Invest. 2012;72(3):221–229.

[26] Wang Z, Chen Z, Li B, et al. Curcumin attenuates renal interstitial fibrosis of obstructive nephropathy by suppressing epithelial-mesenchymal transition through inhibition of the TLR4/NF-κB and PI3K/AKT signalling pathways. Pharm Biol. 2020;58(1):828–837.

[27] Nakamichi M, Akishima-Fukasawa Y, Fujisawa C, et al. Basic fibroblast growth factor induces angiogenic properties of fibrocytes to stimulate vascular formation during wound healing. Am J Pathol. 2016;186(12):3203–3216.

[28] Ashley SL, Wilke CA, Kim KK, et al. Periostin regulates fibrocyte function to promote myofibroblast differentiation and lung fibrosis. Mucosal Immunol. 2017;10(2):341–351.

[29] Xu J, Cong M, Park TJ, et al. Contribution of bone marrow-derived fibrocytes to liver fibrosis. Hepatobiliary Surg Nutr. 2015;4(1):34–47.

[30] Williams SM, Golden-Mason L, Ferguson BS, et al. Class I HDACs regulate angiotensin II-dependent cardiac fibrosis via fibroblasts and circulating fibrocytes. J Mol Cell Cardiol. 2014;67:112–125.

[31] Harris DA, Zhao Y, LaPar DJ, et al. Inhibiting CXCL12 blocks fibrocyte migration and differentiation and attenuates bronchiolitis obliterans in a murine heterotopic tracheal transplant model. J Thorac Cardiovasc Surg. 2013;145(3):854–861.

[32] Roy LD, Sahraei M, Schettini JL, et al. Systemic neutralization of IL-17A significantly reduces breast cancer associated metastasis in arthritic mice by reducing CXCL12/SDF-1 expression in the metastatic niches. BMC Cancer. 2014;14:225.